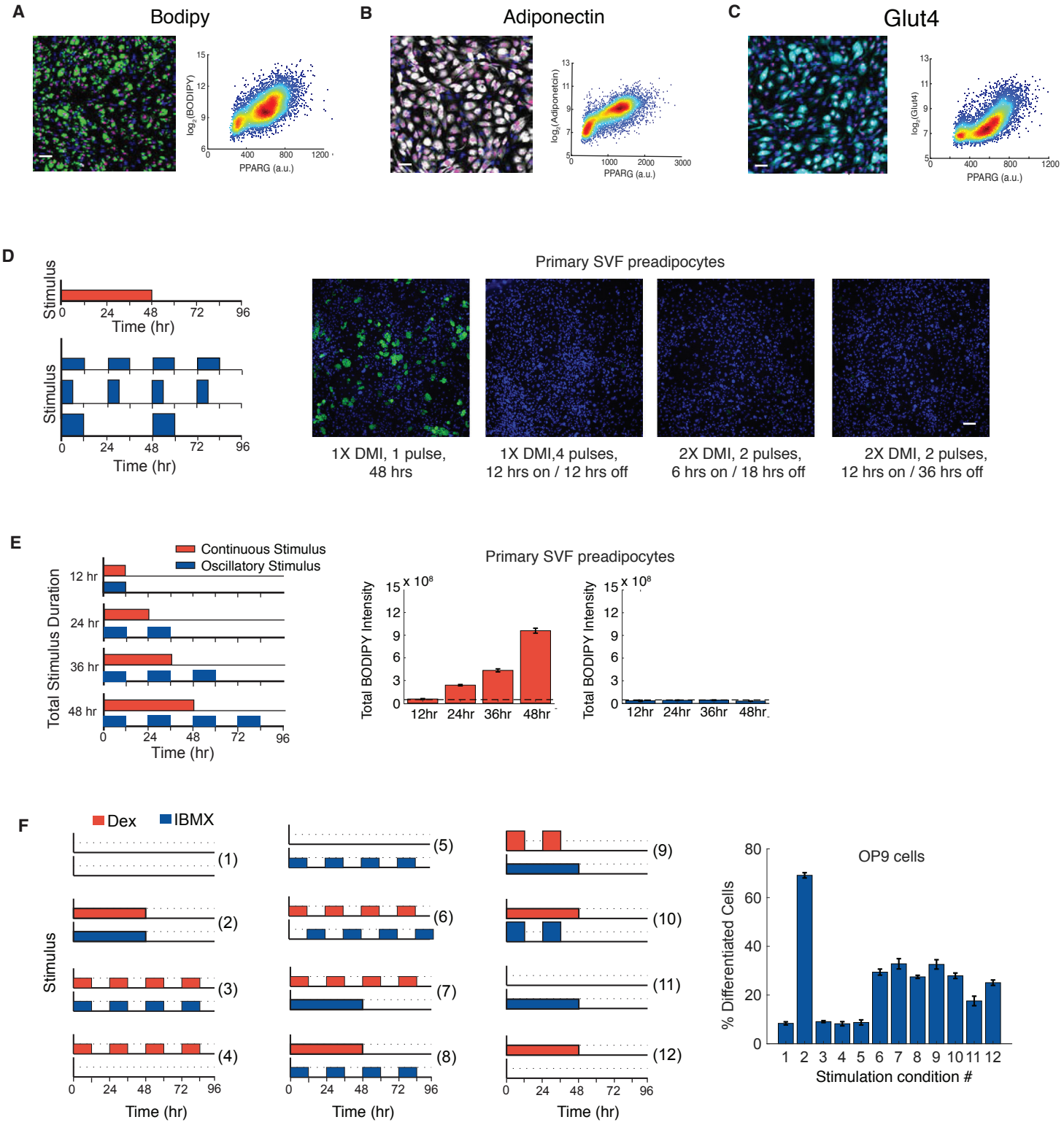


**Figure S1. Adipogenesis creates two populations of cells with either low PPARG (undifferentiated cells) or high PPARG (differentiated cells) and the rejection of circadian hormonal pulses occurs also in primary SVF preadipocytes, Related to Figure 1.**

(A-C) The standard 48hr DMI stimulus was applied at t=0 hrs to mouse OP9 cells. At t=96 hours, the cells were fixed and stained with Hoescht (blue) to mark nuclei and anti-PPARG (red), plus either (A) BODIPY (green), (B) anti-Adiponectin (white), or (C) anti-GLUT4 (turquoise). Images and scatter plots show that the high PPARG correlates closely with lipid accumulation (BODIPY) and markers of mature adipocytes (Adiponectin and GLUT4).

(D-E) Primary SVF preadipocytes treated with the same pulse protocols as in Figure 1D and 1E show the same rejection of circadian hormonal pulses and the same gradual increase in adipogenesis for increasing continuous stimuli with durations greater than 12 hours.

(A,B,C,E) Scale bar represents 20 μm.

(F) Preadipocytes filter both pulses of glucocorticoids (dexamethasone) and cAMP (cellular increase mediated by IBMX). Dexamethasone (1 μM) and/or IBMX (250 μM) were added and removed for the indicated durations of time to cell media consisting of MEMalpha with Pen-Strep, L-glutamine, and 1.75nM insulin.

(D-F) Pulses of stimuli were applied and differentiation was quantitated as described in Figures 1B-1E.

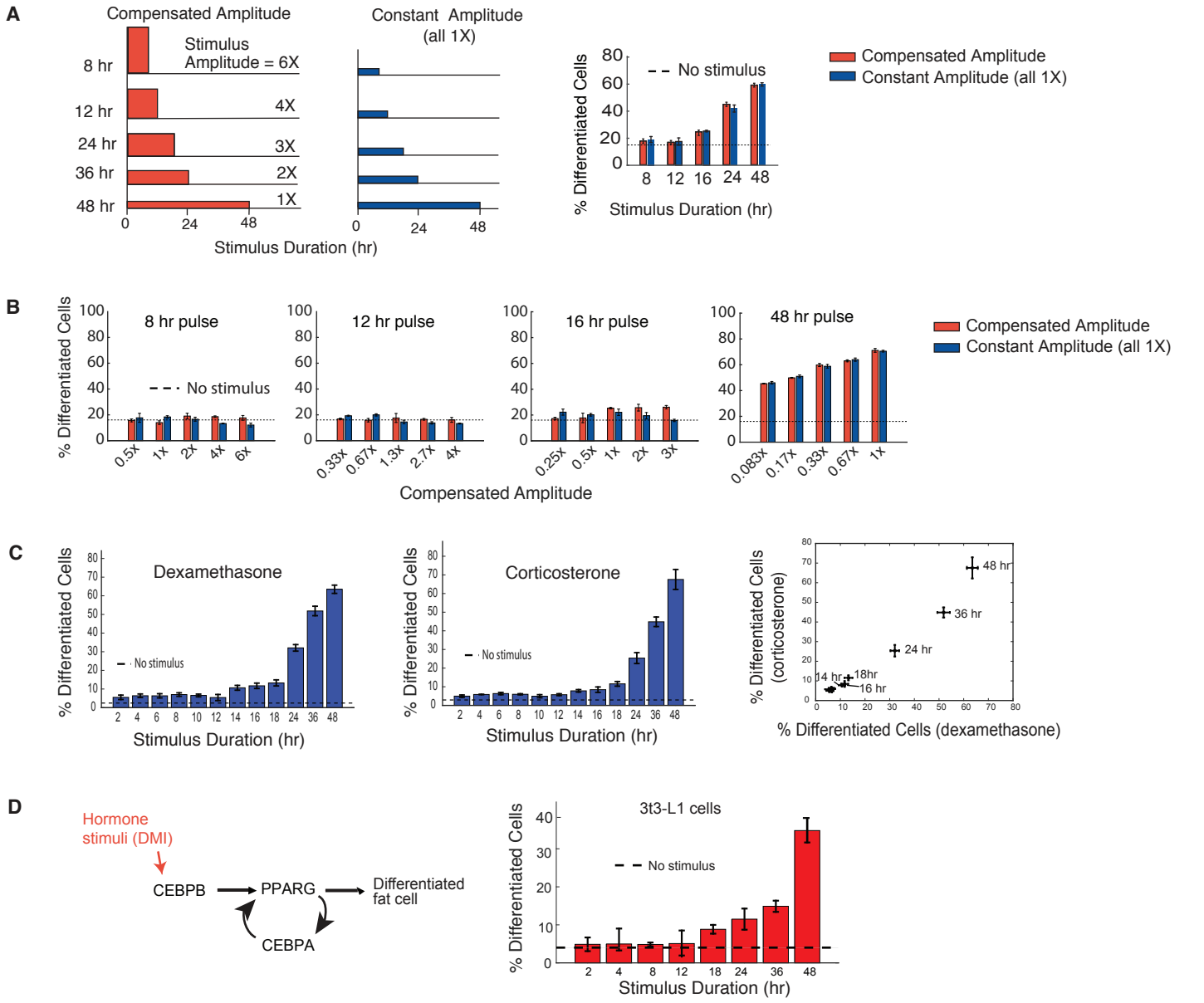


**Figure S2. Verifying that the concentration of the applied DMI pulses is not saturating and that using corticosterone, a physiological glucocorticoids, instead of dexamethasone has the same filtering effect. Also, like OP9 cells, 3T3-L1 cells filter out short and circadian glucocorticoid input signals, Related to Figures 1 and 2.**

(A) Test of whether the rate of preadipocyte differentiation is controlled by the integrated strength of the stimulus or simply by the stimulus duration within a wide-range of stimulus amplitudes. (Left) Schematic showing tested protocols in which DMI stimuli was applied to OP9 preadipocyte cells for different durations at a single concentration (blue) versus at increasing concentrations that kept the total stimulus exposure constant (red). As an example of the latter, if the pulse durations were decreased by two-fold, the pulse amplitudes were increased two-fold to compensate. The cells were fixed 96 hours after application of the stimulus. (Right) Bar plots showing percent of differentiated cells for each protocol. The results show that the same rejection of differentiation stimuli less than 12 hours in duration and graded increase in differentiation rates for stimuli longer than 12 hours is seen whether or not the stimulus amplitude is increased to keep the integrated strength of the stimulus constant.

(B) Verification that the DMI stimulus concentration used is not saturating for pulsatile stimuli. The constant amplitude (1X) of the DMI stimulus was varied across a 12-fold range. Strikingly, the filtering of short duration stimuli was observed for all dilutions tested for both compensated (red bars) and constant 1X (blue bars) amplitude conditions. In contrast, increased differentiation was observed with increasing amplitudes for long 48-hour duration stimuli.

(A-B) In all experiments, the 1X concentration of DMI used was 1 μM dexamethasone, 250 μM IBMX, and 1.76 nM insulin.

(C) Using a physiological glucocorticoid, corticosterone, shows the same differentiation ability and filtering behavior as when the synthetic glucocorticoid, dexamethasone, is used. Stimuli pulses of different durations were applied to OP9 cells to indirectly activate PPARG via activation of the glucocorticoid receptor and CEBPB (DMI). For the corticosterone experiments, 1 μM corticosterone was used instead of 1 μM dexamethesone in the normal DMI stimulus. The results plotted as barplots (left and middle) or in a single scatter plot (right) show that pulsing with corticosterone has the same filtering behavior as pulsing with dexamethasone.

(D) Bar plots showing percent of differentiated cells 96 hours after different durations of stimuli were applied to 3T3-L1 cells to initiate adipogenesis by indirectly activating PPARG via activation of the glucocorticoid receptor and CEBPB upstream of PPARG expression using DMI.

(A,B,C,D) Percent of differentiated cells, measured at 96 hours as in Figure 1B, represents mean +/- s.e.m from 3 technical replicates with approximately 7000 cells per replicate. All data shown are representative of 3 independent experiments.

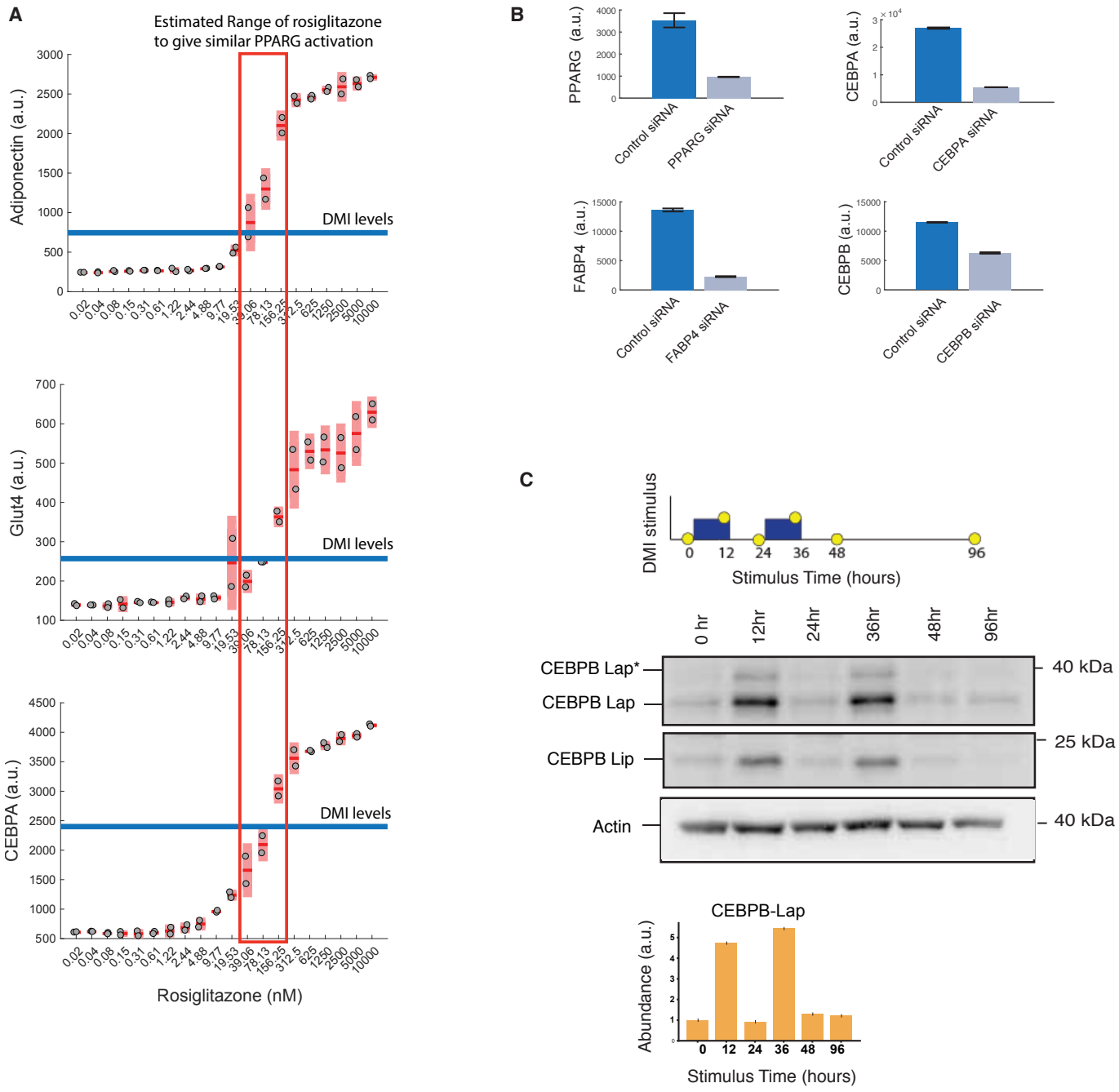


**Figure S3. Determining the concentration of rosiglitazone that gives comparable PPARG activation as a DMI stimulus and measuring CEBPB and PPARG dynamics by western blots, Related to Figure 2.**

(A) To estimate a level of rosiglitazone that gives similar PPARG activation as DMI, different amounts of rosiglitazone were added to the media of undifferentiated mouse OP9 cells plated in 96-well wells in order to induce the cells to differentiate. Forty-eight hours when the cells were maximally differentiated by rosiglitzone, the cells were fixed and stained for Adiponectin, Glut4, and CEBPA protein levels. The titration curves show that ~40 to 100 nM of rosiglitazone for 48 hours matches the expression of the respective genes induced by the standard DMI differentiation protocol (marked by the blue vertical lines). Thus, a dose of 100nM rosiglitazone was used in Figure 2A in order to compare differentiation effects to those resutling from a DMI stimulus. Shaded regions represent 95% confidence interval, and red lines indicate the median value of the duplicate points (grey dots).

(B) Knockdown efficiency of siRNA for PPARG, CEBPA, FABP4, and CEBPB in OP9 cells. Protein levels were assessed by fixing cells immunohistochemistry Error bars show mean intensity +/- s.e.m. from 3 technical replicates, with approximately 8000 cells per technical replicate.

(C) The average CEBPB concentrations in OP9 cells pulsed with DMI were measured by western blot. The barplots show a quantification of the western blots measured using ImageJ analysis software.

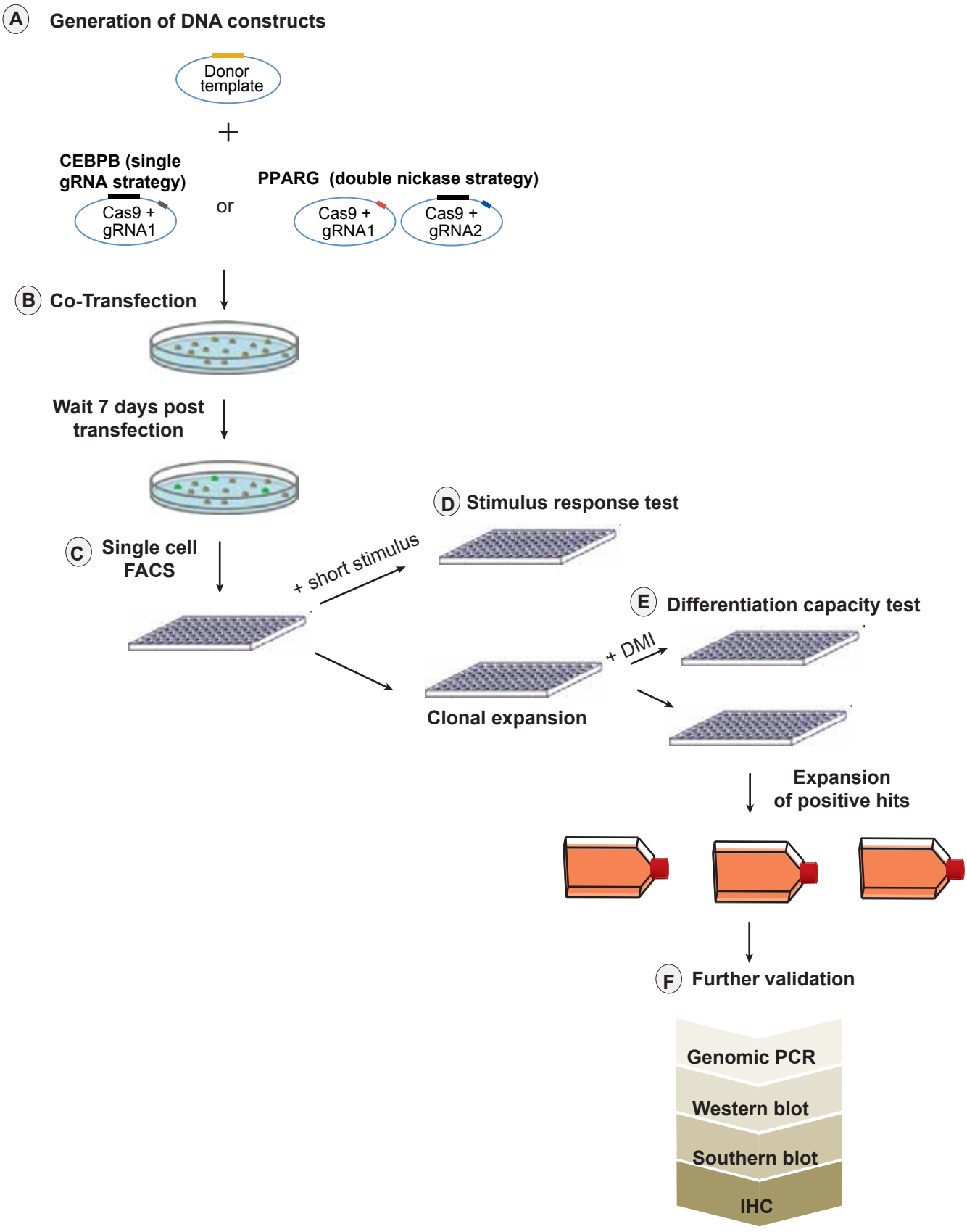


**Figure S4. Workflow for generating and validating single clones with endogenously tagged CEBPB and PPARG using CRISPR-mediated genome editing, Related to Figures 2 and 3.**

The different steps in the workflow are described in detail in the Methods section.

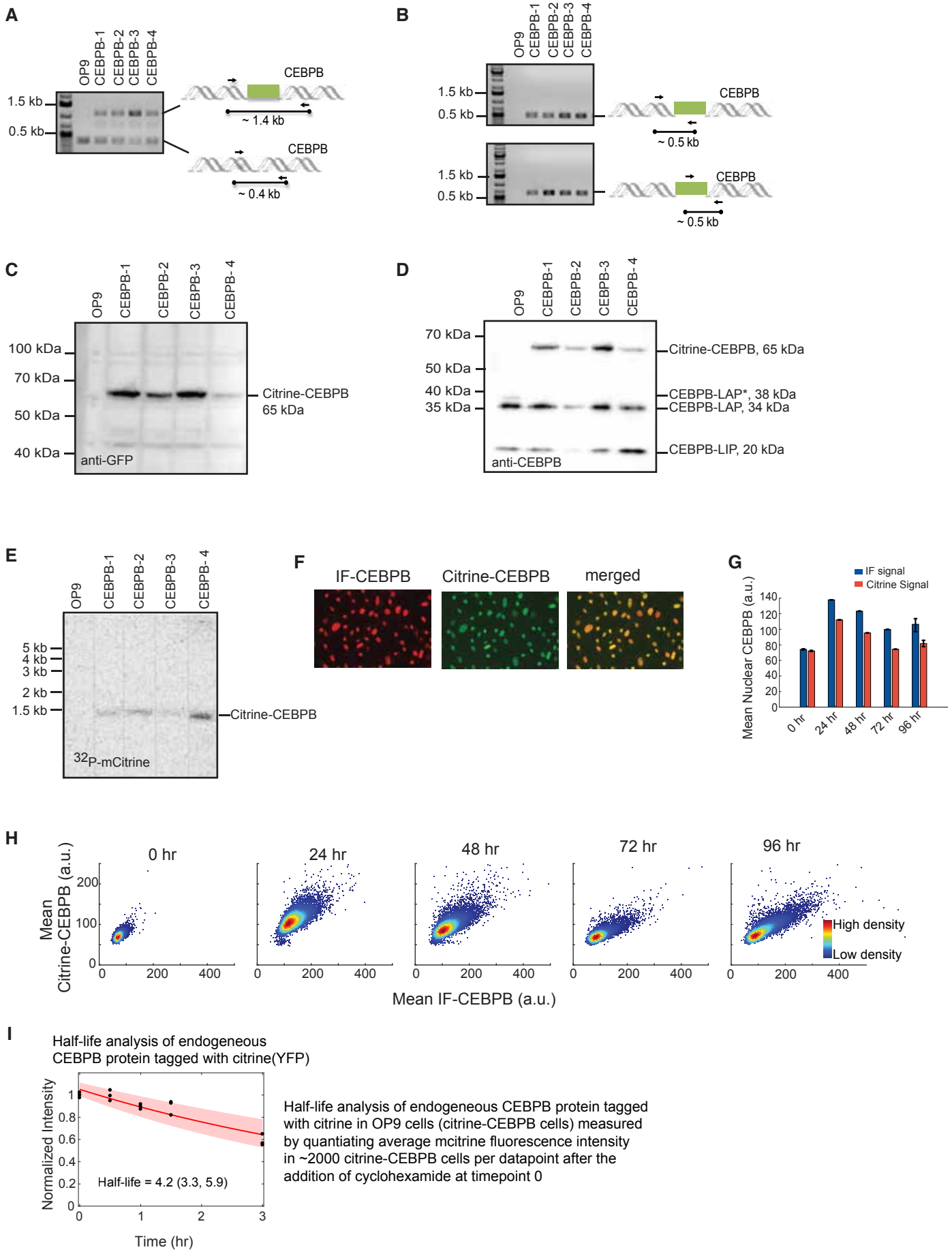


**Figure S5. Validation of CEBPB clones, Related to Figure 2.** The different steps of the validation are described in detail in the Methods section.

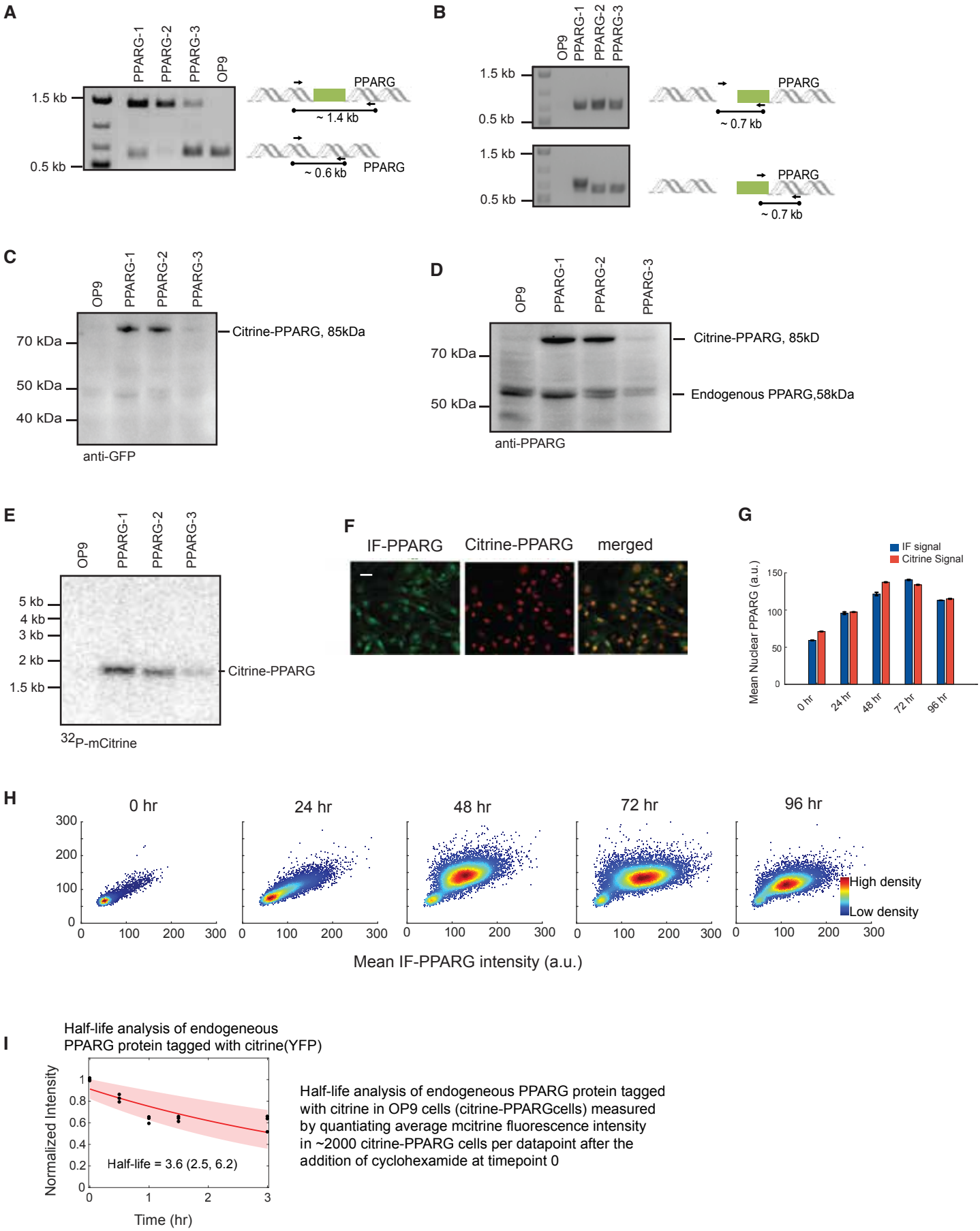


Half-life analysis of endogeneous PPARG protein tagged with citrine in OP9 cells (citrine-PPARGcells) measured by quantiating average mcitrine fluorescence intensity in ~2000 citrine-PPARG cells per datapoint after the addition of cyclohexamide at timepoint 0

**Figure S6. Validation of PPARG clones, Related to Figure 3.** The different steps of the validation are described in detail in the Materials and Methods section.

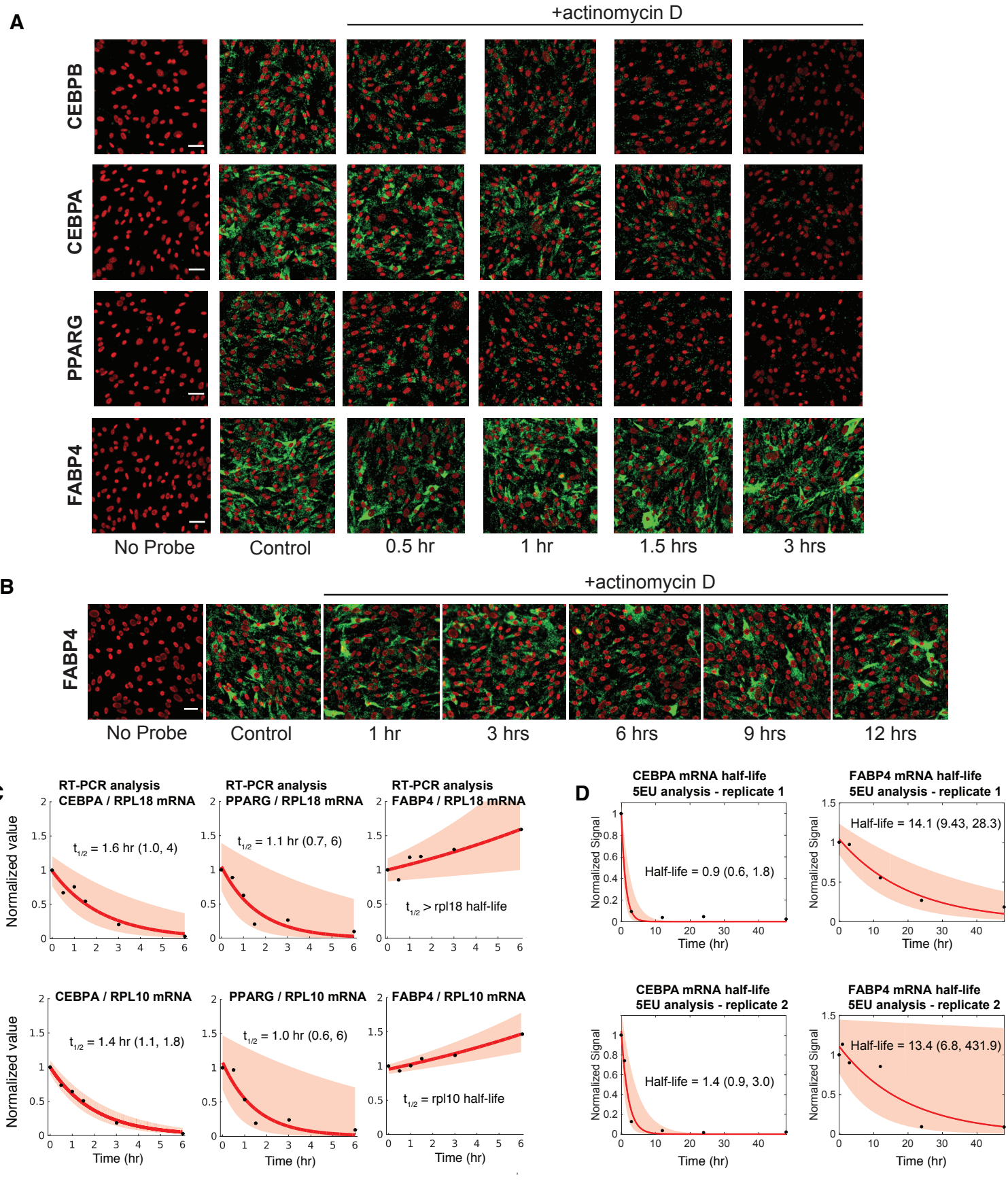


**Figure S7. Measurements of mRNA half-life of CEBPB, CEBPA, PPARG, and FABP4, Related to Figures 2, 3, 4, and 5.**
(A-B) RNA FISH images after the addition of actinomycin D at timepoint 0. The long half-life of FABP4 is apparent by eye, even before carrying out quantiative analysis. Scale bars are 50 μm.
(C) RT-PCR measurements of the levels of CEBPA, PPARG, and FABP4 mRNA ratioed over the levels of the mRNA of RPL18 and RPL10, two long-lived ribosomal proteins, after the addition of actinomycin-D at timepoint 0. These RT-PCR measurements confirm the half-life measurements obtained by RNA FISH.
(D) 5EU measurements of the levels of CEBPA and FABP4 mRNA.

| Target | Strand | Oligonucleotide sequence (5′ to 3′) |
|---|---|---|
| PPARG_Nterm_1 | Top | *CACC*GAGATTTGCTGTAATTCACAC |
| PPARG_Nterm_1 | Bottom | *AAAC*GTGTGAATTACAGCAAATCTC |
| PPARG_Nterm_2 | Top | *CACC*GCTGTTATGGGTGAAACTCT |
| PPARG_Nterm_2 | Bottom | *AAAC*AGAGTTTCACCCATAACAGC |
| CEBPB_Nterm | Top | *CACC*GCGCGTTCATGCACCGCCTGC |
| CEBPB_Nterm | Bottom | *AAAC*GCAGGCGGTGCATGAACGCGC |

**Table S1: Oligonucleotide sequences used to insert sgRNA sequences into the px335 or px330 expression vector, Related to Figures 2 and 3.** Guide sequences are targeted to the PPARG and CEBPB N-terminal. The underlined and italicized nucleotides denote the overhang for ligation of the oligonucleotide duplex into the px335 or px330 guide sequence insertion site.

| Primer Name | Template | Primer sequence (5′ to 3′) |
|---|---|---|
| PPARG_homology_region1_FWD | OP9 genomic DNA | AACCAATTCAGTCGACTGGATCCA AGGCCTTAAGCAAGAAGCC |
| PPARG_homology_region1_REV | OP9 genomic DNA | ACAGCTCCTCGCCCTTGCTCACCA TGGTAAGAACAGCATAAAACAGAG ATTTGCTGTA |
| PPARG_homology_region2_FWD | OP9 genomic DNA | CGAGCTGTACAAGGGAGGAGGAG GTGAAACTCTGGGAGATTCTCC |
| PPARG_homology_region2_REV | OP9 genomic DNA | ATCTCGAGTGCGGCCGCGAATTC GAAATAGAGAATGCAACAT |
| PPARG_Citrine_FWD | Citrine plasmid | TACAGCAAATCTCTGTTTTATGCTG TTCTTACCATGGTGAGCAAGGGCG AGGAGCTGT |
| PPARG_Citrine_REV | Citrine plasmid | CTTGTACAGCTCGTCCATGCCGA |
| CEBPB_homology_region1_FWD | OP9 genomic DNA | AACCAATTCAGTCGACTGCGTTTG TCTCTGATGAC |
| CEBPB _homology_region1_REV | OP9 genomic DNA | ATGGTGGCGAACGCGGGGCC |
| CEBPB_homology_region2_FWD | OP9 genomic DNA | AGGAGGACACCGCCTGCTG |
| CEBPB _homology_region2_REV | OP9 genomic DNA | TCGAGTGCGGCCGCGACCTTCTTC TGC |
| CEBPB _Citrine_FWD | Citrine plasmid | CGCGTTCGCCACCATGGTGAGCA AGGGCGA |
| CEBPB _Citrine_REV | Citrine plasmid | AGGCGGTGTCCTCCTCCCTTGTAC AGCTCGTC |

**Table S2: Primers used for PCR amplification of fragments that were joined by Gibson assembly to create donor vectors to insert Citrine at the N-terminals of PPARG and CEBPB via homologous recombination, Related to Figures 2 and 3.**

| Assay | Primer sequence (5′ to 3′) | Amplicon (bp) |
|---|---|---|
| genotyping PPARG Citrine clones | **FWD:** CAC AGA ACA GTG AAT GTG TGG GTC | **630** (wt allele) |
| | **REV:** GGA AAT GGA AGC CAT GAG CAG | **1347** (knock-in allele) |
| genotyping CEBPB Citrine clones | **FWD:** CTT ATA AAC CTC CCG CTC GGC | **360** (wt allele) |
| | **REV:** AAG AGG TCG GAG AGG AAG TCG T | **1077** (knock-in allele) |

**Table S3: Primers used for genomic PCR analysis of the PPARG and CEBPB CRISPR clones, Related to Figures 2 and 3.**

| Assay | Primer sequence (5′ to 3′) | Amplicon (bp) |
|---|---|---|
| seq. 1<br>PPARG Citrine clones | **FWD:** CAC AGA ACA GTG AAT GTG TGG GTC<br>**REV:** CTT CAG CTC GAT GCG GTT CA | - (wt allele)<br>**717** (knock-in allele) |
| seq. 2<br>PPARG Citrine clones | **FWD:** CAA GGA GGA CGG CAA CAT C<br>**REV:** GGA AAT GGA AGC CAT GAG CAG | - (wt allele)<br>**650** (knock-in allele) |
| seq. 1<br>CEBPB Citrine clones | **FWD:** CTT ATA AAC CTC CCG CTC GGC<br>**REV:** CTT CAG CTC GAT GCG GTT CA | - (wt allele))<br>**475** (knock-in allele) |
| seq. 2<br>CEBPB Citrine clones | **FWD:** CAA GGA GGA CGG CAA CAT C<br>**REV:** AAG AGG TCG GAG AGG AAG TCG T | - (wt allele)<br>**603** (knock-in allele) |

**Table S4: Primers used for genomic PCR analysis to verify the fluorophore integration sites of the PPARG and CEBPB tagged clones, Related to Figures 2 and 3.**

| **Primer Name** | **Primer sequence**<br><br>**(5′ to 3′)** |
|---|---|
| Citrine_probe_FWD | CGACGTAAACGGCCACAAGTT |
| Citrine_probe_REV | ATGGGGGTGTTCTGCTGGTAGT |

**Table S5: Primers used for the PCR amplification of a 504 bp probe directed towards Citrine, Related to Figures 2 and 3.**

| Primer Name | Primer sequence (5′ to 3′) |
|---|---|
| PPARG Fwd | TCGCTGATGCACTGCCTATG |
| PPARG Rev | GAGAGGTCCACAGAGCTGATT |
| CEBPA Fwd | CAAGAACAGCAACGAGTACCG |
| CEBPA Rev | GTCACTGGTCAACTCCAGCAC |
| CEBPB Fwd | CCGGATCAAACGTGGCTGA |
| CEBPB Rev | GATTACTCAGGGCCCGGCTG |
| FABP4 Fwd | AAGGTGAAGAGCATCATAACCCT |
| FABP4 Rev | TCACGCCTTTCATAACACATTCC |
| RPL10 Fwd | CGTGGTGTCCCTGATGCTAAG |
| RPL10 Rev | GTTGGCACAAATACGGGCAG |
| RPL18 Fwd | ATGATGTGCGGATTCTGGAAG |
| RPL18 Rev | CCTGGGGCCTTGCCAAAAT |

**Table S6: Primers used for RT-PCR to measure mRNA degradation rates, Related to Figures 2, 3, 4, and 5.**

| | CONTROL PELLET | CORT PELLET | CONTROL INJECTION | CORT INJECTION |
|---|---|---|---|---|
| **BODY WEIGHT GAIN (G)** | 3.32 ± 0.28 | 4.67 ± 0.56 | 1.08 ± 0.33 | 1.62 ± 0.14 |
| **BODY WEIGHT GAIN (% OF INITIAL BODY WEIGHT)** | 14.0 ± 1.2 | 20.1 ± 2.5 | 4.4 ± 1.3 | 6.4 ± 0.6 |
| **INGUINAL ADIPOSE MASS (MG)** | 251.6 ± 25.0 | 515.3 ± 65.5 | 258.6 ± 18.6 | 271.6 ± 27.7 |
| **INGUINAL ADIPOSE MASS (% OF FINAL BODY WEIGHT)** | 0.93 ± 0.09 | 1.83 ± 0.21 | 1.00 ± 0.07 | 1.01 ± 0.10 |
| **EPIDIDYMAL ADIPOSE MASS (MG)** | 485.5 ± 37.6 | 1070.2 ± 119.4 | 521.4 ± 43.0 | 538.1 ± 69.3 |
| **EPIDIDYMAL ADIPOSE MASS (% OF FINAL BODY WEIGHT)** | 1.80 ± 0.14 | 3.81 ± 0.38 | 2.02 ± 0.16 | 2.01 ± 0.25 |
| **TOTAL FOOD INTAKE OVER THE 26-DAY EXPERIMENTAL TIMECOURSE (G/MOUSE)** | 73.9 | 70.9 | 68.2 | 74.0 |

**Table S7. Summary of experiments described in Figure 7 in which circulating Corticosterone (Cort) levels are manipulated in mice using either implanted Cort pellets or daily Cort injections, Related to Figure 7.** Values are mean +/- s.e.m**.**